

## Nanoscale anisotropic structural correlations in the paramagnetic and ferromagnetic phases of $\text{Nd}_{0.5}\text{Sr}_{0.5}\text{MnO}_3$

V. Kiryukhin,<sup>1</sup> B. G. Kim,<sup>1</sup> T. Katsufuji,<sup>2</sup> J. P. Hill,<sup>3</sup> and S-W. Cheong<sup>1,2</sup>

<sup>1</sup>*Department of Physics and Astronomy, Rutgers University, Piscataway, New Jersey 08854*

<sup>2</sup>*Bell Laboratories, Lucent Technologies, Murray Hill, New Jersey 07974*

<sup>3</sup>*Department of Physics, Brookhaven National Laboratory, Upton, New York 11973*

(Received 24 October 2000; revised manuscript received 3 January 2001; published 16 March 2001)

We report x-ray scattering studies of short-range structural correlations and diffuse scattering in  $\text{Nd}_{0.5}\text{Sr}_{0.5}\text{MnO}_3$ . On cooling, this material undergoes a series of transitions, first from a paramagnetic insulating (PI) to a ferromagnetic metallic (FM) phase, and then to a charge-ordered (CO) insulating state. Highly anisotropic structural correlations were found in both the PI and FM states of this compound. The correlations increase with decreasing temperature, reaching a maximum at the CO transition temperature. Below this temperature, they abruptly collapsed. Single-polaron diffuse scattering was also observed in both the PI and FM states suggesting that substantial local lattice distortions are present in these phases. We argue that our measurements indicate that nanoscale regions exhibiting layered orbital order exist in the paramagnetic and ferromagnetic phases of  $\text{Nd}_{0.5}\text{Sr}_{0.5}\text{MnO}_3$ .

DOI: 10.1103/PhysRevB.63.144406

PACS number(s): 75.30.Vn, 71.38.-k, 71.30.+h

Manganite perovskites of the chemical formula  $A_{1-x}B_x\text{MnO}_3$  (where  $A$  is a rare earth, and  $B$  is an alkali earth atom) have recently attracted considerable attention because they exhibit a number of interesting electronic properties, including the colossal magnetoresistance phenomenon.<sup>1</sup> Recent studies show convincingly that a number of the intriguing properties of the manganites cannot be understood through spatially uniform phases and that local inhomogeneities must play an essential role in these compounds.<sup>2</sup> The high resistivity of the paramagnetic insulating (PI) phase found in most of the manganites at high temperatures, for example, results in part from the presence of the lattice polarons that form when an  $e_g$  electron localizes on a  $\text{Mn}^{3+}$  site, inducing the Jahn-Teller distortion of the  $\text{MnO}_6$  octahedron.<sup>3</sup> Such lattice polarons were recently detected directly in the PI phase of the manganites by means of diffuse x-ray and neutron scattering.<sup>4,5</sup> Magnetic and lattice polarons have also been found in other phases of the manganites, including the ferromagnetic metallic (FM) and insulating, and antiferromagnetic insulating phases.<sup>5,6</sup>

The properties of the high-temperature paramagnetic insulating phase were recently found to exhibit sharp anomalies at several commensurate concentrations of doped carriers, such as  $x=3/8$  and  $x=1/2$ .<sup>7</sup> The presence of these anomalies suggested that local charge or orbital correlations of some kind, possibly short-range polaron-polaron correlations, play an important role in the PI phase. Recently, such polaron correlations were indeed observed in  $\text{La}_{1-x}\text{Ca}_x\text{MnO}_3$ ,  $\text{La}_{2-2x}\text{Sr}_{1+2x}\text{Mn}_2\text{O}_7$ , and  $\text{Pr}_{1-x}\text{Ca}_x\text{MnO}_3$  manganites.<sup>4,5</sup> Interestingly, the high-temperature structural correlations do not necessarily correspond to the low-temperature order, and in some cases the incipient high-temperature ordering is in direct competition with the ground state.<sup>5</sup> The relationship between the low-temperature ground state and the high-temperature correlations is at present largely unclear.

While local structural correlations appear to play an important role in the macroscopically homogeneous states of

the manganites, the microscopic nature of these correlations, as well as the extent to which they affect the electronic properties of the manganites, have yet to be established. To answer these questions, extensive experimental and theoretical work is needed.

In this paper, we report synchrotron x-ray scattering studies of short-range structural correlations and diffuse scattering in  $\text{Nd}_{0.5}\text{Sr}_{0.5}\text{MnO}_3$ . We find a new type of correlated anisotropic lattice distortion in the ferromagnetic and paramagnetic phases of this material. We argue that these correlated distortions are associated with local regions of layered orbital and, possibly, magnetic order. These observed structural correlations then provide a natural explanation for the anisotropic magnetic properties of this three-dimensional perovskite compound.

Single crystals of  $\text{Nd}_{0.5}\text{Sr}_{0.5}\text{MnO}_3$  were grown using the standard floating zone technique. The x-ray diffraction measurements were carried out at beamlines X22A and X20C at the National Synchrotron Light Source. In each case, the x-ray beam was focused by a mirror, monochromatized by a Si (111) monochromator, scattered from the sample mounted inside a closed-cycle cryostat, and analyzed with a pyrolytic graphite crystal. In this paper, Bragg peaks are indexed in the orthorhombic  $Ibmm$  notation in which the longest lattice constant is  $c$ .

$\text{Nd}_{0.5}\text{Sr}_{0.5}\text{MnO}_3$  is a paramagnetic insulator at high temperatures. With decreasing temperature, it undergoes a transition to a ferromagnetic metallic state at  $T_c=250$  K, and at  $T_{CO}=150$  K, it becomes a CE-type charge ordered insulator possessing the  $d_{3x^2-r^2/3y^2-r^2}$  type orbital ordering.<sup>8</sup> In addition, weak magnetic Bragg peaks due to the presence of an  $A$ -type antiferromagnetic impurity phase, in which ferromagnetic layers are stacked antiferromagnetically along the (001) direction, have been observed in some samples below  $T_{AF}=200$  K.<sup>9</sup> Finally, in some of the samples studied previously, these phases were found to coexist with the higher-temperature phases either below  $T_{AF}$  or below  $T_{CO}$ .<sup>10</sup> Note,

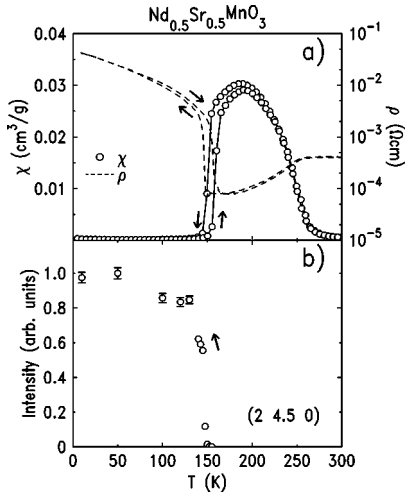


FIG. 1. (a) Temperature dependence of the zero-field electrical resistivity (dashed line) and the magnetic susceptibility (open circles) in a magnetic field of 2000 Oe. (b) The intensity of the (2, 4.5, 0) peak characteristic of the CE-type charge and orbitally ordered state.

these samples were all found to consist of a single structural phase at temperatures higher than 200 K.

The bulk properties of our sample are consistent with the results published in the literature. Figure 1 shows the temperature dependence of the magnetic susceptibility, electrical resistivity, and the intensity of the (2, 4.5, 0) peak, which is characteristic of the CE-type charge and orbitally ordered state. From the data of Fig. 1, we obtain  $T_c \approx 260$  K, and  $T_{CO} \approx 150$  K. There is a measurable hysteresis in the magnetic susceptibility below  $T \approx 200$  K, and therefore it is possible that the sample contains several structural phases at low temperatures, as was reported in Ref. 10.

In order to characterize the short-range structural correlations and the single-polaron diffuse scattering, we have measured the x-ray intensity in the vicinity of several representative Bragg peaks. Figure 2 shows a contour plot of the x-ray intensity in the vicinity of the (4, 0, 0) and the (4, 2, 0) Bragg points. The crystals are twinned in all the three cubic directions of the underlying cubic perovskite structure, and therefore the data of Fig. 2 consist of a superposition of the scattering due to all the twin domains in the crystal. In particular, in the top panel of Fig. 2, the Bragg reflections (4, 0, 0) and (2, 2, 4) coincide, and scattering from both the ( $hk0$ ) and the ( $hhl$ ) zones is present. Similarly, the Bragg reflections (4, 2, 0), (3, 3, 2), and (1, 1, 6), and combined scattering from the ( $hk0$ ) and ( $hhl$ ) zones are present in the bottom panel of Fig. 2. The main coordinate axes in this figure show the ( $hk0$ ) zone; the axes for the ( $hhl$ ) zone are superimposed on the figure.

The data of Fig. 2 exhibit intense, anisotropic, and very broad scattering at the (4.5, 1.5, 0), (3.5, 2.5, 0), and (4.5,  $\pm 0.5$ , 0) points in the ( $hk0$ ) axes setting.<sup>11</sup> Alternatively, this scattering can be ascribed to the (3, 3, 3), (3, 3, 1), and (2, 2, 5) reciprocal space coordinates. For a reason that will become clear later, we will use the latter assignment, in which the scattering occurs with a (0, 0, 1) reduced scattering vector. Note, for crystal with  $Ibmm$  symmetry, as

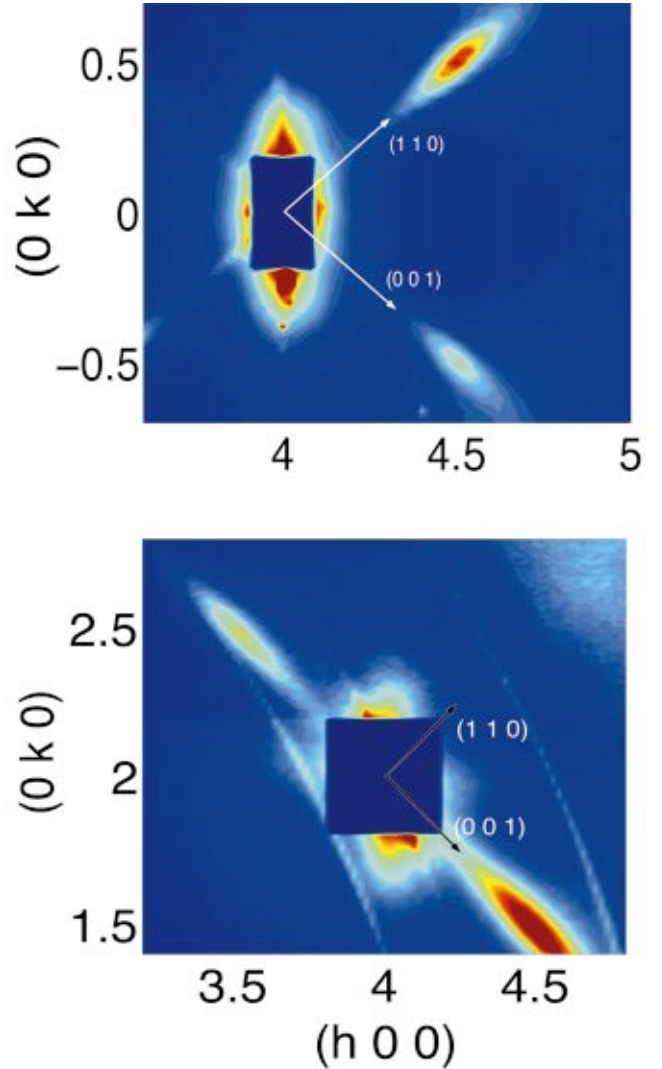


FIG. 2. (Color) Contour plots of the scattered x-ray intensity around the (4, 0, 0) Bragg peak at  $T=165$  K (top panel), and around the (4, 2, 0) peak at  $T=270$  K (bottom panel). (See the text for the explanation of the effects of twinning.) The two light circular arcs in the bottom panel are due to impurity powder scattering.

$\text{Nd}_{0.5}\text{Sr}_{0.5}\text{MnO}_3$  has at temperatures higher than  $T_{CO}$ ,<sup>8,10</sup> the (3,3,3), (3,3,1), and (2,2,5) reflections are forbidden. We have studied the temperature dependence of the scattering at these points. Scans were taken along the (00 $l$ ), ( $hh0$ ), and ( $h-h0$ ) directions. The data collected in the ( $hh0$ ) and ( $h-h0$ ) scans were essentially identical, and in what follows we will not distinguish them, simply referring to them as scans perpendicular to the (00 $l$ ) direction. Examples of the scans in the (00 $l$ ) direction at the (3, 3, 3) reciprocal lattice point are shown in the inset in Fig. 3. To parametrize the data, the scans were fitted to a Lorentzian to the power 1.5 lineshape convoluted with the instrumental resolution, and the resulting fits were used to extract the peak intensities and the intrinsic peak widths.

Because the diffracted x-ray intensity is proportional to the square of the Fourier transform of the atomic density-density correlation function, the broad peaks of Fig. 2 signal

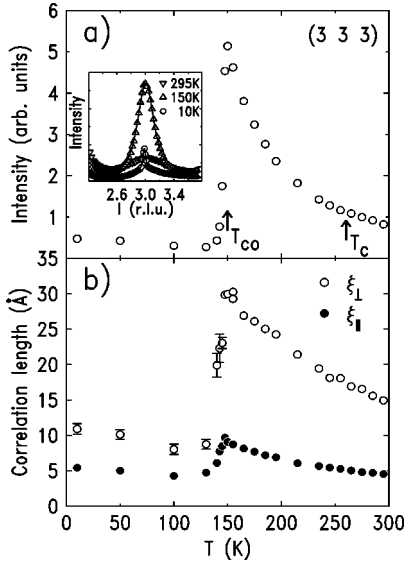


FIG. 3. Temperature dependence of the x-ray intensity of the (3, 3, 3) peak (a), and of the correlation lengths of the corresponding structural fluctuations (b).  $\xi_{\perp}$  is the correlation length perpendicular to the reduced scattering vector (001) and  $\xi_{\parallel}$  is the correlation length parallel to this vector (the “in-plane” and “out-of-plane” correlation lengths). The inset in (a) shows scans through the (3, 3, 3) peak, along the (00 $l$ ) direction at different temperatures.

the presence of correlated lattice distortions above  $T_{CO}$ . The anisotropic correlation length (the domain size) of these regions can be extracted from the intrinsic width of the peaks and is shown in Fig. 3 along with the temperature dependence of the x-ray intensity at the (3, 3, 3) reciprocal lattice point. We find that the correlation length is approximately 3 times smaller in the (001) direction than in the perpendicular direction at all temperatures. As the temperature decreases, both correlation lengths grow and reach their maximum at a temperature just above  $T_{CO}$ . The scattering then abruptly collapses at  $T_{CO} \approx 150$  K. Below  $T_{CO}$ , two components in the scattering are observed, a sharp component and a broad component (inset in Fig. 3). The integrated intensity of the sharp component was approximately 100 times smaller than the integrated intensity of the correlations measured at  $T = 150$  K, and was approximately independent of temperature below  $T = 150$  K. The possible multiphase character of the low-temperature state makes it hard to assign these observed components to specific phases.

The large anisotropy of the structural correlations observed above  $T = 150$  K makes it natural to propose that they correspond to the lattice distortions arising from the presence of some kind of layered orbital order in the correlated domains. One possible scenario is that these correlated domains possess the layered  $d_{x^2-y^2}$ -type orbital order<sup>8</sup> and exhibit the associated  $A$ -type antiferromagnetism. This scenario is supported by a recent observation of anisotropic spin fluctuations in  $\text{Nd}_{0.5}\text{Sr}_{0.5}\text{MnO}_3$  by means of neutron scattering.<sup>9</sup> These spin fluctuations exhibited two-dimensional character in the PM phase, and were of the antiferromagnetic  $A$  type in the FM phase.<sup>9</sup> In addition,  $\text{Nd}_{1-x}\text{Sr}_x\text{MnO}_3$  samples with  $x > 0.51$  exhibit the  $A$ -type antiferromagnetic metallic (AFM)

low-temperature state, and therefore strong AFM fluctuations can be expected in the  $x = 0.5$  compound which lies close to the AFM phase boundary. In the above picture of the correlations, the reduced wave vector of the structural distortion characteristic of the correlated domains in our sample, (0, 0, 1), is perpendicular to the FM layers, and the periodicity of the lattice modulation is twice the distance between these layers.<sup>12</sup>

It is also possible that the structural correlations of Fig. 2 reflect the gradual change of the crystal structure from the  $Pbnm$  symmetry for low Sr concentrations to the  $Ibmm$  symmetry for  $x > 0.5$ . [The (3, 3, 3), (3, 3, 1), and (2, 2, 5) peaks are allowed in the  $Pbnm$  space group.] These two structures exhibit different patterns of the tilts of  $\text{MnO}_6$  octahedra.<sup>8,10</sup> The  $Pbnm$  symmetry is normally found in the FM and CE-type states in the manganites,<sup>1</sup> while the  $Ibmm$  symmetry is characteristic to the layered  $A$ -type AFM state in  $\text{Nd}_{1-x}\text{Sr}_x\text{MnO}_3$ . The structural features characteristic to the latter lattice symmetry therefore favor the  $A$ -type state with the associated orbital and magnetic order. The gradual conversion of the  $Pbnm$  structure to the  $Ibmm$  structure with increasing  $x$  can proceed in a variety of possible ways. Spatial phase separation can, for example, take place. A more interesting scenario of a uniform average structure exhibiting fluctuating correlated  $Pbnm$  domains is also plausible. We note that our study, as well as the results of Refs. 8,10, do not support the presence of phase separation for  $T > 200$  K. Independent on the exact microscopic structure of our sample, the pronounced anisotropy of the  $Pbnm$ -type correlations shows that in the correlated domains, the coupling in the  $ab$  planes is much stronger than the interplane coupling. Since the  $ab$  planes form the ferromagnetic layers in the  $A$ -type AFM state for  $x > 0.5$ , it is likely that the diminished interlayer coupling found in the  $x = 0.5$  compound reflect the incipient  $A$ -type layered orbital order. In the above scenario, therefore, the presence of the anisotropic lattice fluctuations provide an *indirect* evidence of the local layered orbital order in the PM and the FM phases.

Our preliminary diffraction measurements on  $\text{Nd}_{0.7}\text{Sr}_{0.3}\text{MnO}_3$  samples indicate the presence of weak Bragg peaks characteristic to the  $Pbnm$  symmetry group. To determine which of the two scenarios described above is correct, however, it is necessary to perform detailed structural studies of the  $\text{Nd}_{1-x}\text{Sr}_x\text{MnO}_3$  samples for a number of Sr concentration in the vicinity of  $x = 0.5$ . In particular, the possible structural fluctuations should be investigated in the AFM state itself and in its immediate vicinity. This work is currently in progress.

We believe that the newly observed type of structural correlations cannot be attributed to small admixtures of the  $A$ -type AFM or of the charge-ordered phases with the PI or the FM phases for three reasons. First, at temperatures higher than  $T = 200$  K,  $\text{Nd}_{0.5}\text{Sr}_{0.5}\text{MnO}_3$  samples are believed to consist of a single structural phase.<sup>8,10</sup> Secondly, the data of Fig. 3 do not show any obvious anomaly at  $T_{AF}$ . Finally, the (0, 0, 1)-type scattering abruptly disappears below  $T_{CO}$ . We conclude that these correlations are therefore intrinsic features of the PI and the FM phases.

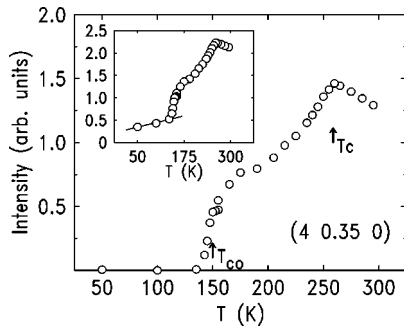


FIG. 4. Temperature dependence of the single-polaron diffuse scattering at a scattering vector  $Q=(4, 0.35, 0)$ . The estimated phonon contribution, which is shown as a solid line in the inset, is subtracted. The inset shows the raw data.

Finally, we briefly discuss the x-ray diffuse scattering observed in the vicinity of the main Bragg peaks. Such scattering is clearly visible in the data of Fig. 2 as an elongated oval shape around the Bragg peak in the top panel, and as a “butterflylike shape” in the bottom panel. It has been previously demonstrated that diffuse scattering of this kind results from the presence of uncorrelated lattice polarons.<sup>4</sup> The symmetry of the diffuse scattering in Fig. 2 is consistent with the measurements reported in Refs. 4,5, and we therefore also interpret its intensity as reflecting the number of single polarons present in the sample.

Figure 4 shows the temperature dependence of this single-polaron diffuse scattering at a scattering vector  $Q=(4, 0.35, 0)$ , that is on the wing of the oval shape in the top panel of Fig. 2. The phonon contribution to the diffuse scattering was estimated from the data for  $T < T_{CO}$  (Ref. 13) and subtracted. The remaining part, which reflects the polaron contribution, shows a number of interesting features. First, the number of polarons grows with decreasing temperature in the PI phase, in agreement with Refs. 4,5. At  $T_c$ , the intensity turns around and starts to fall. At  $T_{CO}$ , the uncorrelated polarons abruptly disappear—as would be expected following the formation of long-range orbital order. We note that the concen-

tration of single polarons does *not* exhibit an abrupt drop at  $T_c$ , and the polarons are clearly present in the FM phase. In contrast to this behavior, polaron scattering intensity abruptly decreases upon the transition to the FM state in  $\text{La}_{0.7}\text{Ca}_{0.3}\text{MnO}_3$  and  $\text{La}_{1.8}\text{Sr}_{1.8}\text{Mn}_2\text{O}_7$ , compounds which are believed to possess a microscopically uniform FM phase.<sup>4,5</sup> In  $\text{Nd}_{0.5}\text{Sr}_{0.5}\text{MnO}_3$ , *both* the uncorrelated polarons and the correlated anisotropic lattice distortions are present below the Curie temperature, and therefore the FM phase of this material is clearly less uniform than the FM phase of the former compounds (see also Ref. 9). Unlike the intensity of the (3, 3, 3) peak, the intensity of the single-polaron scattering shows a clear anomaly at  $T_c$ . It appears, therefore, that the anisotropic lattice distortions discussed above are not directly coupled with the system of the disordered lattice polarons.

In summary, we report observation of anisotropic short-range correlated structural distortions in the paramagnetic insulating phase and the ferromagnetic metallic phase of  $\text{Nd}_{0.5}\text{Sr}_{0.5}\text{MnO}_3$ . We argue that the observed structural correlations indicate the presence of local layered orbital order in our samples. Together with the anisotropy of the magnetic excitations reported in Ref. 9, these structural inhomogeneities show that the ferromagnetic and paramagnetic phases of  $\text{Nd}_{0.5}\text{Sr}_{0.5}\text{MnO}_3$  are nonuniform and exhibit large structural and magnetic fluctuations which, possibly, reflect the incipient layered magnetic order characteristic to the  $\text{Nd}_{1-x}\text{Sr}_x\text{MnO}_3$  samples with  $x > 0.51$ . Combined with the results of previous work, our observations strongly suggest that short-range structural correlations associated with local regions of orbital and magnetic order play an important role in magnetoresistive manganite materials.

We are grateful to M. Croft, D. Gibbs, C. S. Nelson, and M. v. Zimmermann for important discussions. This work was supported by the NSF under Grant No. DMR-9802513, by Rutgers University, and by the U.S. Department of Energy under Contract No. AC02-98CH10886.

<sup>1</sup>For a review, see *Colossal Magnetoresistance Oxides*, edited by Y. Tokura (Gordon & Breach, London, 1999).

<sup>2</sup>M. Uehara, S. Mori, C. H. Chen, and S-W. Cheong, *Nature (London)* **399**, 560 (1999); S. J. L. Billinge, R. G. DiFrancesco, G. H. Kwei, J. J. Neumeier, and J. D. Thompson, *Phys. Rev. Lett.* **77**, 715 (1996); D. Louca, T. Egami, E. L. Brosha, H. Röder, and A. R. Bishop, *Phys. Rev. B* **56**, R8475 (1997); S. Yunoki, J. Hu, A. L. Malvezzi, A. Moreo, N. Furukawa, and E. Dagotto, *Phys. Rev. Lett.* **80**, 845 (1998).

<sup>3</sup>A. J. Millis, P. B. Littlewood, and B. I. Shraiman, *Phys. Rev. Lett.* **74**, 5144 (1995); A. Alexandrov and A. M. Bratkovsky, *ibid.* **82**, 141 (1999).

<sup>4</sup>L. Vasiliu-Doloc, S. Rosenkranz, R. Osborn, S. K. Sinha, J. W. Lynn, J. Mesot, O. H. Seeck, G. Preosti, A. J. Fedro, and J. F. Mitchell, *Phys. Rev. Lett.* **83**, 4393 (1999); S. Shimomura, N. Wakabayashi, H. Kuwahara, and Y. Tokura, *ibid.* **83**, 4389

(1999); S. Shimomura, T. Tonegawa, K. Tajima, N. Wakabayashi, N. Ikeda, T. Shobu, Y. Noda, Y. Tomioka, and Y. Tokura, *Phys. Rev. B* **62**, 3875 (2000).

<sup>5</sup>Pengcheng Dai, J. A. Fernandez-Baca, N. Wakabayashi, E. W. Plummer, Y. Tomioka, and Y. Tokura, *Phys. Rev. Lett.* **85**, 2553 (2000); C. P. Adams, J. W. Lynn, Y. M. Mukovskii, A. A. Arsenov, and D. A. Shulyatev, *ibid.* **85**, 3954 (2000); C. S. Nelson, M. v. Zimmermann, J. P. Hill, D. Gibbs, V. Kiryukhin, T. Y. Koo, S-W. Cheong, D. Casa, B. Keimer, Y. Tomioka, Y. Tokura, T. Gog, and C. T. Venkataraman, cond-mat/0011502 (unpublished).

<sup>6</sup>J. M. DeTeresa, M. R. Ibarra, P. A. Algarabel, C. Ritter, C. Marquina, J. Blasco, J. Garcia, A. del-Moral, and Z. Arnold, *Nature (London)* **386**, 256 (1997); M. Hennion, F. Moussa, G. Biotteau, J. Rodriguez-Carvajal, L. Pinsard, and A. Revcolevschi, *Phys. Rev. B* **61**, 9513 (2000).

- <sup>7</sup>K. H. Kim, M. Uehara, and S-W. Cheong, *Phys. Rev. B* **62**, R11 945 (2000).
- <sup>8</sup>R. Kajimoto, H. Yoshizawa, H. Kawano, H. Kuwahara, Y. Tokura, K. Onoyama, and M. Ohashi, *Phys. Rev. B* **60**, 9506 (1999).
- <sup>9</sup>H. Kawano, R. Kajimoto, H. Yoshizawa, Y. Tomioka, H. Kuwahara, and Y. Tokura, cond-mat/9808286 (unpublished); H. Yoshizawa, R. Kajimoto, H. Kawano, J. A. Fernandez-Baca, Y. Tomioka, H. Kuwahara, and Y. Tokura, *Mater. Sci. Eng., B* **B63**, 125 (1999).
- <sup>10</sup>P. M. Woodward, D. E. Cox, T. Vogt, C. N. R. Rao, and A. K. Cheetham, *Chem. Mater.* **11**, 3528 (1999); C. Ritter, R. Mahendiran, M. R. Ibarra, L. Morellon, A. Maignan, B. Raveau, and C. N. R. Rao, *Phys. Rev. B* **61**, R9229 (2000).
- <sup>11</sup>One possible reason for the absence of the (4.5, 2.5, 0) and (3.5, 1.5, 0) reflections in the data of Fig. 2 could be that the displacements of atoms in the correlated domains are predominantly transverse [perpendicular to the (001) direction]: for a small displacement,  $\delta$  of an atom from its average position, the x-ray intensity is proportional to  $|\mathbf{Q} \cdot \delta|^2$ , where  $\mathbf{Q}$  is the scattering vector.
- <sup>12</sup>Note, lattice constant  $c$  in the orthorhombic  $Ibmm$  space group is twice as large as the corresponding lattice constant of cubic perovskite lattice.
- <sup>13</sup>We assumed that this contribution is linear with temperature, see B. E. Warren, *X-Ray Diffraction* (Addison-Wesley, Reading, MA, 1969).